Korean J. Chem. Eng., 35(12), 2474-2479 (2018)
DOI: 10.1007/s11814-018-0179-5

pISSN: 0256-1115
eISSN: 1975-7220

Characteristics of NiO films prepared by atomic layer deposition using bis(ethylcyclopentadienyl)-Ni and O_2 plasma

Su-Hyeon Ji, Woo-Sung Jang, Jeong-Wook Son, and Do-Heyoung Kim†

School of Chemical Engineering, Chonnam National University, Gwangju 61186, Korea
(*Received 4 September 2018 • accepted 23 October 2018*)

Abstract−Plasma-enhanced atomic layer deposition (PEALD) is well-known for fabricating conformal and uniform films with a well-controlled thickness at the atomic level over any type of supporting substrate. We prepared nickel oxide (NiO) thin films via PEALD using bis(ethylcyclopentadienyl)-nickel ($Ni(EtCp)_2$) and O_2 plasma. To optimize the PEALD process, the effects of parameters such as the precursor pulsing time, purging time, O_2 plasma exposure time, and power were examined. The optimal PEALD process has a wide deposition-temperature range of 100-325 °C and a growth rate of 0.037±0.002 nm per cycle. The NiO films deposited on a silicon substrate with a high aspect ratio exhibited excellent conformality and high linearity with respect to the number of PEALD cycles, without nucleation delay.

Keywords: Plasma-enhanced Atomic Layer Deposition, Atomic Layer Deposition, Nickel Oxide, Thin Film, Bis(ethylcyclopentadienyl)-nickel

INTRODUCTION

Nickel oxide (NiO) is a promising material for various industrial applications, including photovoltaics, catalysis, and energy storage devices, because of its distinguished features, which include high conductivity, excellent electroactivity, and good redox activity and chemical stability [1,2]. The preparation of NiO over an uneven feature-substrate via an appropriate deposition technique is crucial for improving its mechanical stability and performance in those practical applications. Many methods have already been developed for preparing NiO thin films, including sputtering, sol-gel methods, spray pyrolysis, chemical vapor deposition (CVD), and atomic layer deposition (ALD) [3-10]. Among these, ALD has attracted considerable attention as an effective way to prepare high-quality NiO thin films because it can control the film thickness precisely and achieve conformal films with good uniformity over an uneven feature-substrate as a result of the self-limited reaction that occurs on the surface during the ALD process. Furthermore, the ALD process can be performed at lower temperatures than conventional CVD, which allows the facile preparation of thin films [11]. Many ALD reaction systems for synthesizing NiO thin films have been investigated. Nucleation delay and a narrow ALD window are considered to be the drawbacks of reaction systems utilizing $Ni(dmamp)_2$ (dmamp, 1-dimethylamino-2-methyl-2-propanolate) and ($Ni(thd)_2$) (thd, bis(2,2,6,6-tetramethyl-3,5-heptanedionato)Ni(II)) with water [12,13]. To resolve these issues, other processes using nickelocene ($Ni(Cp)_2$) as a precursor and ozone as a reactant have been proposed [14-16]. Although these processes usually had a wider deposition-temperature range (150-300 °C) than those of previous cases, their relatively low saturated growth rate was unfavorable for device applications. To overcome this limitation, a reaction system that utilizes bis(ethylcyclopentadienyl)-nickel [$Ni(EtCp)_2$] with ozone for NiO ALD was recently proposed. Because $Ni(EtCp)_2$ is a liquid precursor under standard temperature and pressure conditions, it allows the facile control of the ALD process and the generation of sufficient amounts of vapor pressure for depositing films in the ALD process compared with a solid precursor. However, it also has drawbacks such as a narrow ALD window and low growth rate [16-18]. From this viewpoint, the plasma-enhanced ALD (PEALD) system is very attractive, because the PEALD process allows a wider ALD window, reducing the deposition temperature compared with the conventional ALD process [19].

Here, for the first time, we report a PEALD process that employs a liquid precursor of $Ni(EtCp)_2$ as a nickel precursor and oxygen (O_2) plasma as a reactant. We systematically investigated the effects of the precursor pulsing time, purging time, O_2 plasma exposure time, and plasma power on the characteristics of the NiO film growth.

EXPERIMENTAL

All the experiments were performed in a homemade vertical-flow shower-head type PEALD chamber using a p-type silicon substrate with a crystal orientation of (100) manufactured by STC (JAPAN). The chamber wall was heated at 100 °C. $Ni(EtCp)_2$ [EtCp= ethylcyclopentadienyl, $(C_2H_5)C_5H_4$] was purchased from DNF Co. and used as a precursor without any purification. The nickel precursor was kept in a stainless container and heated to 50 °C. The delivery line was heated at 60 °C to avoid condensation of the precursor. Argon gas was used as the carrier and purging gas. Oxygen (O_2) gas was used for the O_2 plasma system, and a flow rate of 150 sccm was maintained during the experiment. A radiofrequency controller (RFX-600, 13.56 MHz) was used to generate O_2 plasma. One deposition cycle consisted of the precursor pulsing (30 sccm), main purging (30 sccm), bypass purging (250 sccm), oxygen plasma

†To whom correspondence should be addressed.
E-mail: kdhh@chonnam.ac.kr

exposure (150 sccm, 50 W), and Ar purging (250 sccm), which occurred in sequence. The purpose of the Ar purging was to remove the excess reactant between the precursor pulsing and O_2 plasma steps. The main purging and bypass purging employed different flow rates after the precursor pulsing, which were used to effectively remove the excess precursor present in the homemade vertical-flow shower-head type PEALD system.

Prior to the experiment, a silicon wafer was dipped in a diluted hydrofluoric acid solution for 1 min to eliminate the natural SiO_2 layers. Then, the substrates were cleaned with acetone, isopropyl alcohol, and deionized water for 1 min, sequentially. Lastly, the substrates were dried with N_2.

To optimize the PEALD process and obtain uniform films, we examined the effects of many different parameters such as the precursor pulsing time, precursor purging time, bypass purging time, oxygen plasma time, and purging time. As a result, the pulse time of $Ni(EtCp)_2$ was fixed at 1.5 s. The main purging was fixed at 20 s, with bypass purging for 5 s. The O_2 plasma and Ar purging of O_2 plasma steps lasted 5 s and 30 s, respectively. During the PEALD process, the process pressure was 0.44 Torr, with a plasma power of 50 W. Various deposition temperatures in the range of 100-325 °C were used.

The thickness of each as-deposited NiO film was measured using ellipsometry (LSE Stokes ellipsometer (Gaertner Scientific, USA)). The crystallinity of each NiO film was confirmed via grazing incidence X-ray diffraction (GIXRD) measurements (X'Pert Pro using CuKα), and the elemental composition of the obtained films was analyzed using X-ray photoelectron spectroscopy (XPS) measurements (VG Multilab 2000 (Hosmed, Finland)) at the Center for Research Facilities of Chonnam National University. The conformality of the films was investigated via high-resolution scanning electron microscopy (HR-SEM) (Hitachi, Japan) at the Korean Basic Science Institute (KBSI, Gwangju Center). The surface roughness of each prepared film was estimated using atomic force microscopy (AFM) (XE-100). The root-mean-square (RMS) roughness values were calculated using 1 μm×1 μm areas.

RESULTS AND DISCUSSION

First, NiO films were grown on the silicon substrates using

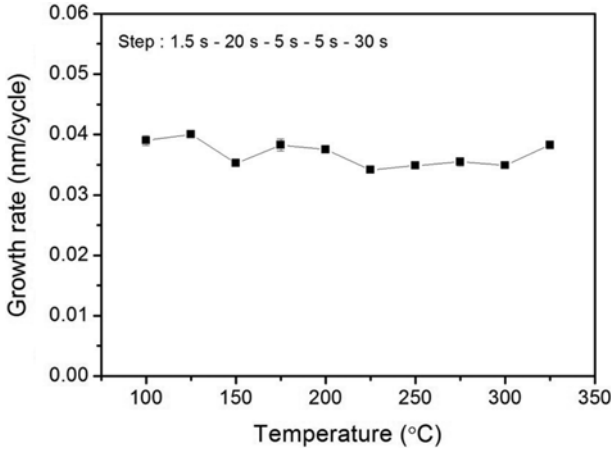

Fig. 1. Growth rate of NiO films using PEALD process as function of deposition temperature.

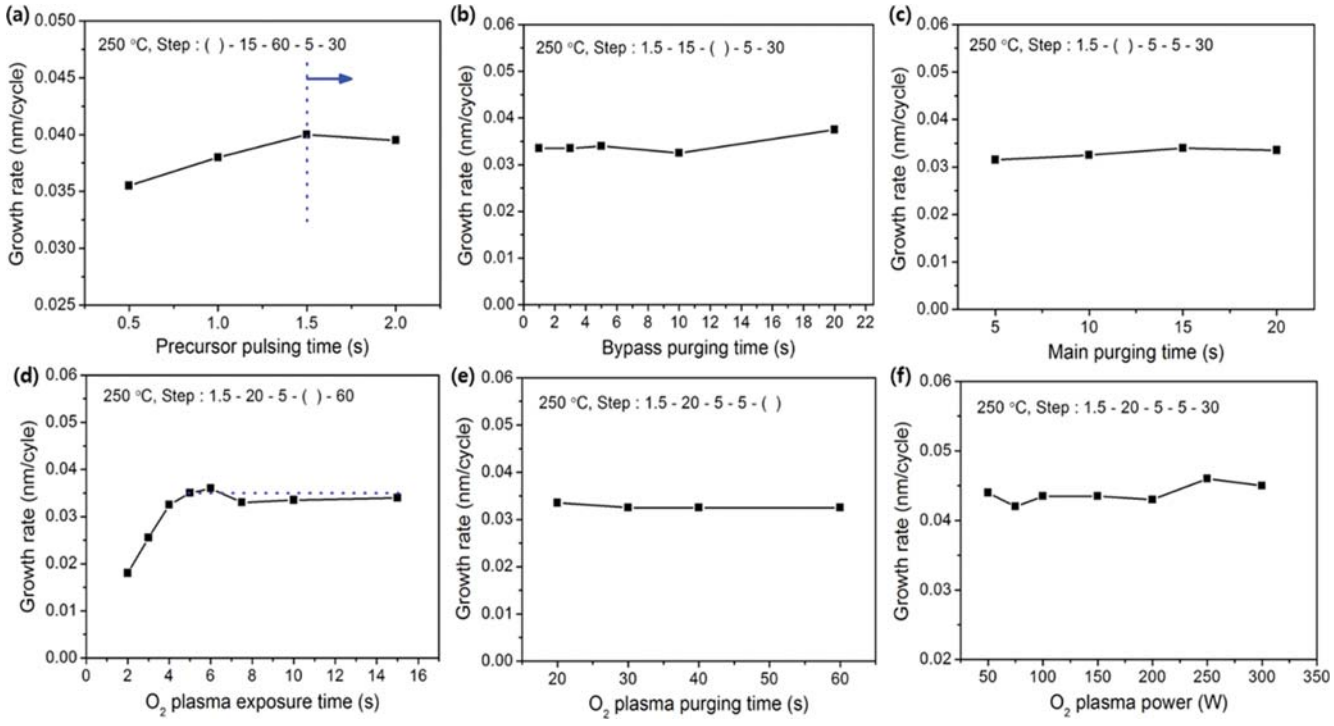

Fig. 2. (a) Growth rates at different Ni pulsing times, with O_2 plasma exposure time fixed at 5 s and power fixed at 50 W. (b), (c) Growth rates of PEALD films with different bypass and main purging times. (d) Growth rates of PEALD films with respect to the O_2 plasma exposure time. (e) Growth rates at different O_2 plasma purging times. (f) Growth rate with respect to the O_2 plasma power.

$Ni(EtCp)_2$ and O_2 plasma to investigate the temperature window of the PEALD process. The NiO films were deposited over a wide temperature range of 100-325 °C. Fig. 1 shows the growth rates of the NiO films for various deposition temperatures. We obtained the saturated growth rate of the thickness for this temperature range (100-325 °C). In this temperature range, the growth rate of the NiO films was 0.037±0.002 nm per cycle. A similar saturated growth rate over a wide temperature range could be utilized for applications involving temperature-sensitive materials.

To optimize the PEALD process, NiO films were deposited at 250 °C while varying different parameters such as the precursor dose time, main purging time, bypass purging time, O_2 plasma exposure time, plasma power, and O_2 plasma purging time, as shown in Fig. 2. Initially, we looked at the effect on the growth rate of different precursor pulsing times while fixing the other conditions, as described below. The main purging lasted 15 s, with bypass purging of 60 s, an O_2 plasma exposure time of 5 s, Ar purging time of 30 s, and 50 W of power. When the precursor pulsing time was increased from 0.5 to 2.0 s, the growth rate also increased until 1.0 s, and then it was saturated over 1.5 s, as shown in Fig. 2(a). To examine the effects of the bypass and main purging times, we evaluated different purging times, as shown in Fig. 2(b) and 2(c), respectively. First, the bypass purging time was considered, because the bypass purging flow (250 sccm) was higher than the main purging flow (30 sccm), which suggested that the bypass purging was more effective at removing excess reactant than the main purging. In Fig. 2(b), we observe that the growth rate was saturated over 1 s, indicating that a bypass purging time of 1 s was sufficient for self-limiting film growth [20]. During this test, the main purging time was set to 5 s. Thus, the main purging time was examined in a similar way. We obtained similar growth rates for times greater than 15 s and fixed the main purging time at 20 s. The effects of the O_2 plasma exposure time, purging time, and plasma power on the growth rate were also evaluated via a similar procedure, as shown in Fig. 2(d)-2(f), respectively. In Fig. 2(d), as the O_2 plasma exposure time increases, the growth rate increases until 5 s, at which point a constant growth rate is observed at times greater than 5 s.

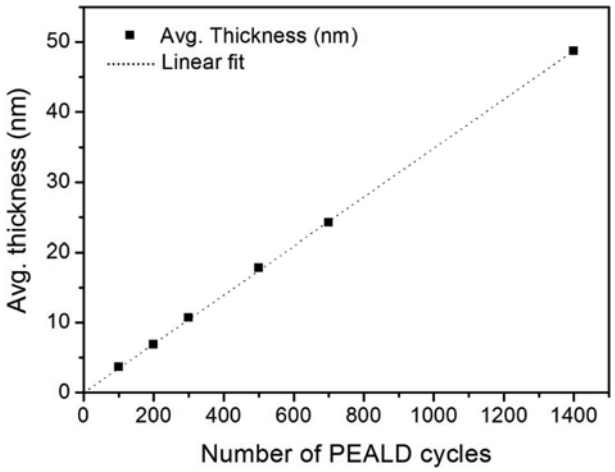

Fig. 3. Average thickness of NiO films deposited at 250 °C on silicon substrates with respect to number of PEALD cycles.

Table 1. Impurities of NiO films (from XPS analysis)

Deposition temperature (°C)	O/Ni ratio	C contents (at%)
100	0.88	1.24
250	0.91	0.49
325	0.90	N.D.*

*N.D.: No detection

A purging time of 30 s was used for the NiO films to avoid contamination, although we obtained a saturated growth rate over a period of 20 s, as shown in Fig. 2(e). Additionally, we examined the effect of the plasma power, and 50 W was found to be sufficient to obtain saturation of the growth rate, as shown in Fig. 2(f). The linearity of the growth rate was evaluated using silicon substrates, as shown in Fig. 3. As the number of PEALD cycles increased, the average thickness of the NiO films increased linearly, without nucleation delay. The growth rate remained constant throughout the PEALD process, allowing us to precisely control the film thickness for device applications.

To investigate the properties of the NiO films, such as the film composition, bonding state, and conformality, with respect to the deposition temperature, we examined NiO films deposited at 100, 250, and 325 °C using several analysis methods, including XPS, GIXRD, and SEM. First, the XPS spectra of the obtained NiO films were studied to elucidate the elemental compositions and bonding states. Prior to the XPS analyses, the as-deposited NiO films were etched for 1 min by Ar ions to remove the outermost layers. The compositions of NiO films deposited at different temperatures are summarized in Table 1. As the deposition temperature increased, the carbon content decreased, and there was no carbon contamination at 325 °C. Fig. 4(a) shows the narrow XPS spectra of Ni 2p for the NiO films deposited at 100, 250, and 325 °C. The maximum peaks of Ni $2p_{3/2}$ and Ni $2p_{1/2}$ are at 853 and 871 eV, respectively. Additionally, there are satellite Ni 2p peaks between Ni $2p_{3/2}$ and Ni $2p_{1/2}$. To obtain detailed information regarding the Ni 2p and O 1s peaks, we analyzed the NiO deposited at 250 °C. Fig. 4(b) shows the XPS full spectrum of NiO films deposited at 250 °C, confirming the presence of Ni and O, along with a small amount of carbon peaks. In Fig. 4(c), we observe two peaks of Ni $2p_{3/2}$ and Ni $2p_{1/2}$, which occur at 853.7 and 871.9 eV, respectively. An analysis of the narrow spectrum of Ni 2p shows that the aforementioned values of Ni $2p_{3/2}$ and Ni $2p_{1/2}$ correspond to the Ni^{2+} of NiO [14]. The satellite peaks of Ni $2p_{3/2}$ and Ni $2p_{1/2}$ are at 861.2 and 879.1 eV, respectively. Fig. 4(d) shows the XPS narrow spectrum of O 1s. There are two deconvoluted peaks in the narrow XPS spectra of O 1s. Out of these, a sharp peak is observed at 529.3 eV, which corresponds to the O^{2-} of NiO. Another peak at 531.2 eV is attributed to the surface hydroxide of the NiO film [14,21].

GIXRD was used to analyze the crystallinity of the NiO films deposited using different parameters, e.g., different numbers of PEALD cycles at 250 °C and various deposition temperatures (100, 250, and 325 °C), as shown in Fig. 5. We evaluated the crystalliniy of the NiO films deposited at different temperatures, as shown in Fig. 5(a). In the case of the NiO films deposited at different temperatures, all the films were amorphous, without any sharp peaks.

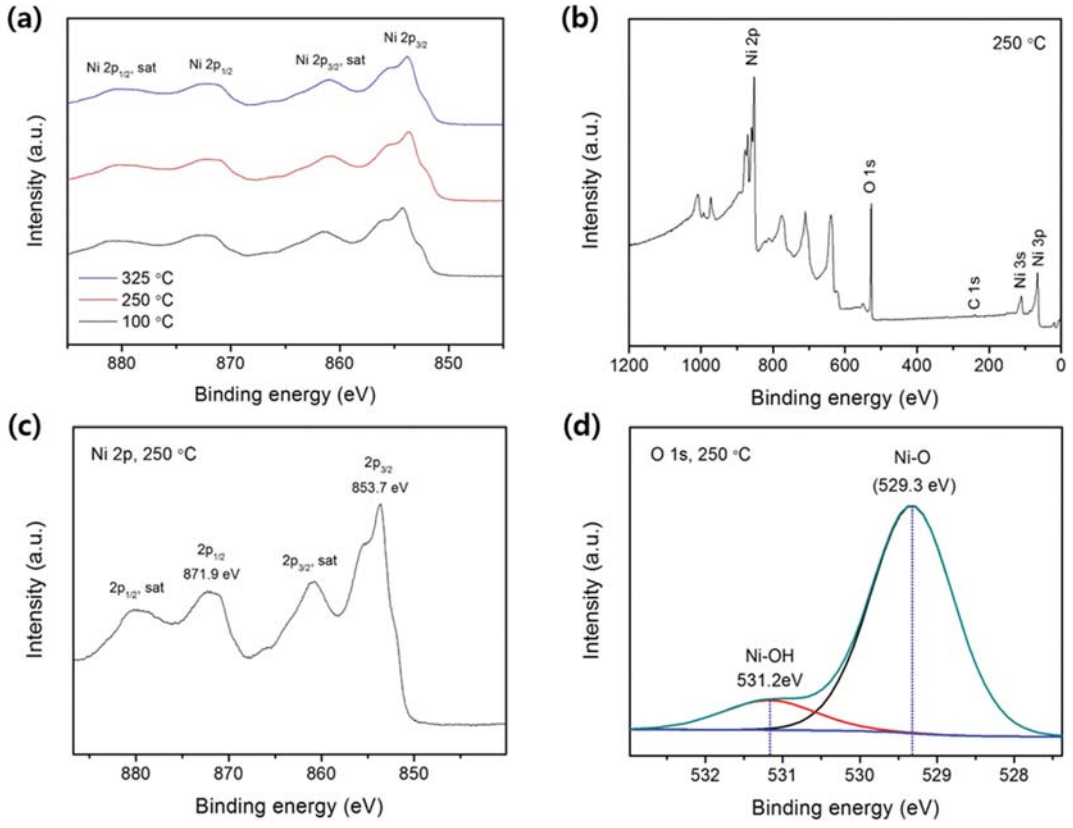

Fig. 4. (a) Narrow XPS spectra of Ni 2p for NiO films deposited at 100, 250, and 325 °C; (b) broad XPS spectra for NiO films deposited at 250 °C; and narrow XPS spectra for Ni 2p (c) and O 1s (d).

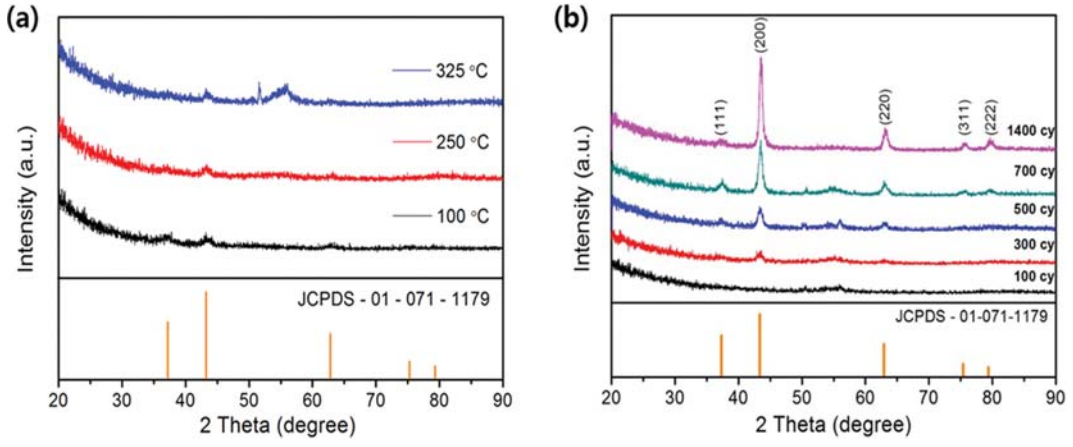

Fig. 5. GIXRD of NiO films deposited on silicon substrates (a) at different deposition temperatures and (b) with different numbers of PEALD cycles at 250 °C.

We did not observe a correlation between the deposition temperature and the crystallinity [20]. Additionally, we analyzed NiO films deposited using different numbers of PEALD cycles at 250 °C, using GIXRD to confirm the crystallinity in relation to the increasing number of cycles, as shown in Fig. 5(b). The GIXRD peaks of the as-deposited films corresponded to the NiO phase (JCPDS - 01-071-1179) [22]. The intensity of the peak increased with the number of PEALD cycles. We confirmed that the growth in the (200) direction was dominant.

Similarly, the surface roughness of each NiO film was measured via AFM, as shown in Fig. 6. Fig. 6(a) shows the results for NiO films deposited at different temperatures with similar average thicknesses of approximately 10 nm. We confirmed that the surface roughness increased with the deposition temperature, which indicated that the crystallinity increased with the deposition temperature [23]. Fig. 6(b) shows how the RMS roughness was affected by increasing the number of PEALD cycles. As the thickness of the NiO film increased, the RMS roughness also increased. Initially,

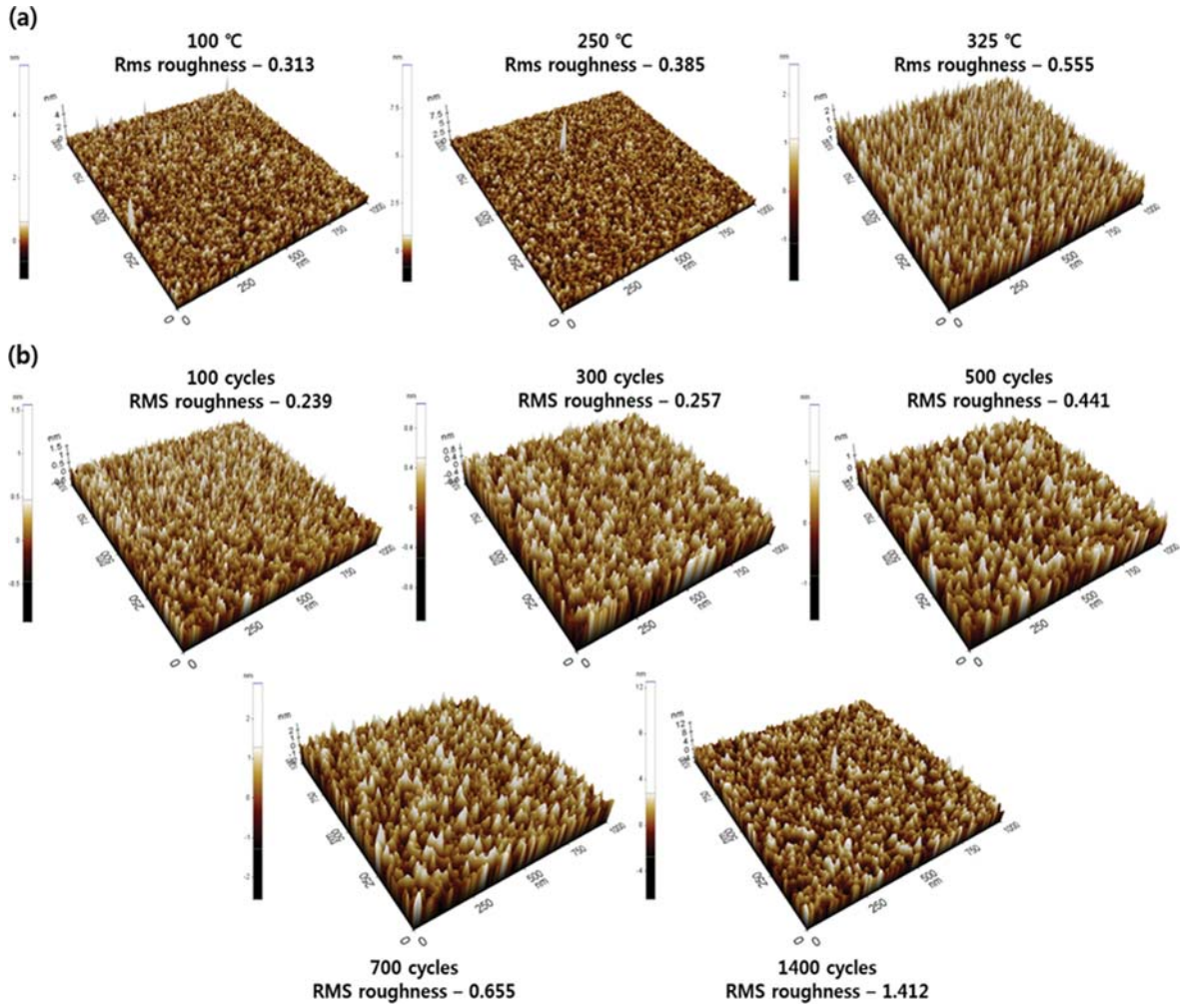

Fig. 6. Atomic force micrographs of NiO films deposited using (a) different deposition temperatures and (b) different numbers of PEALD cycles at 250 °C.

NiO films produced using 100 cycles were very smooth (RMS roughness: 0.239 nm). As the number of PEALD cycles increased to 300, 500, 700, and 1,400, the RMS roughness increased to 0.257, 0.441, 0.655, and 1.412 nm, respectively. These features can be applied in various ways depending on the application. For example, in supercapacitors or lithium-ion batteries, a high film roughness is effective at enhancing the performance [24,25] because it can yield a large surface area, allowing more contact between the active elec-

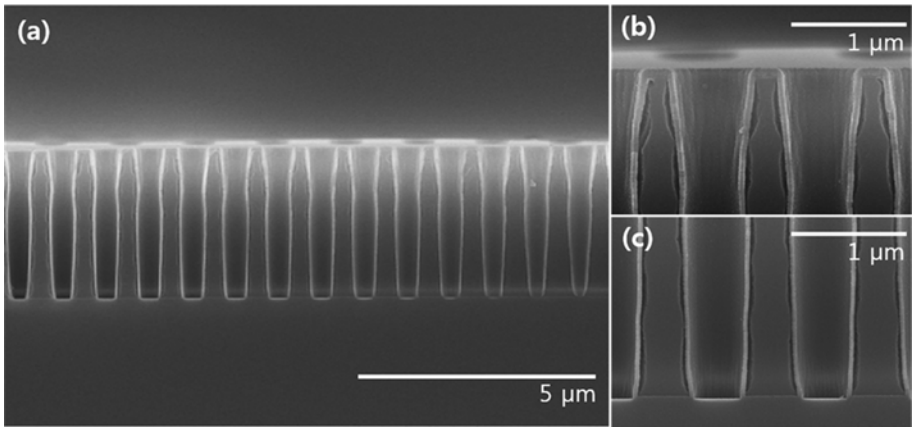

Fig. 7. (a) Cross-sectional SEM image of NiO film deposited at 250 °C using PEALD process; (b), (c) magnified top and bottom images of (a), respectively.

trode materials and the electrolyte. In contrast, for a solar cell, a uniform thin film with a low roughness is important because it can affect the resistance of the device [26]. Therefore, the thickness and surface roughness can be tailored according to the characteristics of the equipment.

The PEALD process is well known to have poor conformality because plasma radicals cause a recombination at the wall of a high-aspect-ratio substrate. Therefore, the conformality and step coverage of the thin films are very important points, allowing the PEALD system to be used for other applications. To examine the conformality and step coverage of the NiO thin films, they were deposited on a high-aspect ratio silicon substrate to a thickness of 25 nm under the optimum PEALD conditions (1.5 s - 20 s - 5 s - 5 s - 30 s) at 250 °C. Fig. 7 shows cross-sectional SEM images of the NiO films, with Fig. 7(b) and 7(c) showing top and bottom views, respectively, of Fig. 7(a). We clearly confirmed that the NiO thin films were uniformly deposited over the top and bottom of the substrate, as shown in Fig. 7(b) and 7(c), respectively, which indicated that the deposited NiO thin films exhibited excellent conformality, and this PEALD system demonstrated excellent step coverage by the uniform good growth on the substrate. These features can yield uniform films on devices with any structure, which will make it possible to improve the performance [27].

CONCLUSION

We demonstrated the use of the PEALD process for NiO using bis(ethylcyclopentadienyl)-nickel [$Ni(EtCp)_2$] as a nickel source and O_2 plasma as a reactant while varying different parameters such as the precursor pulsing time, purging time, and plasma exposure time. We obtained a constant growth rate of 0.037±0.002 nm per cycle in a wide range of temperatures: 100-325 °C. To study the effect of the deposition temperature, NiO films deposited at 100, 250, and 325 °C were analyzed via XPS, XRD, AFM, and so on. The as-deposited films corresponded to the NiO phase, and the presence of NiO was confirmed through XPS. The carbon content decreased with the increasing deposition temperature, and there was no carbon at 325 °C. AFM verified that the film roughness depended on the deposition temperature and number of PEALD cycles at 250 °C. The RMS roughness increased from 0.239 to 1.412 nm when the number of ALD cycles was increased at 250 °C, and RMS roughness values of 0.313, 0.385, and 0.555 nm were obtained at deposition temperatures of 100, 250, and 325 °C, respectively. Cross-sectional SEM showed the excellent conformality of the NiO thin films achieved using a high-aspect ratio patterned wafer. This PEALD process could be used for a variety of applications in accordance with the characterization of the materials.

CONFLICT OF INTEREST

The authors declare no conflicts of interest.

ACKNOWLEDGEMENTS

This research was supported by the National Research Foundation of Korea (NRF-2017R1E1A1A03070930). We thank the Korea Basic Science Institute (KBSI) at Gwangju Center for the analysis.

REFERENCES

1. P. Rai, J. W. Yoon, H. M. Jeong, S. J. Hwang, C. H. Kwak and J. H. Lee, *Nanoscale*, **6**, 8292 (2014).
2. J. Wang, L. Wei, L. Zhang, J. Zhang, H. Wei, C. Jiang and Y. Zhang, *J. Mater. Chem.*, **22**, 20038 (2012).
3. R. Betancur, M. Maymo, X. Elias, L. T. Vuong and J. Martorell, *Solar Energy Mater. Solar Cells*, **95**, 735 (2011).
4. A. A. Al-Ghamdi, W. E. Mahmoud, S. J. Yaghmour and F. M. Al-Marzouki, *J. Alloys Compd.*, **486**, 9 (2009).
5. Z. Zhu, Y. Bai, T. Zhang, Z. Liu, X. Long, Z. Wei, Z. Wang, L. Zhang, J. Wang, F. Yan and S. Yang, *Angew. Chem.*, **126**, 12779 (2014).
6. K. O. Ukoba, A. C. Eloka-Eboka and F. L. Inambao, *Renew. Sust. Energy Rev.*, **82**, 2900 (2018).
7. J. H. Kim, H. M. Lee, D. W. Kang, K. M. Lee and C. K. Kim, *Korean J. Chem. Eng.*, **33**, 9, 2711 (2016).
8. D. Barreca and C. Massignan, *Chem. Mater.*, **13**(2), 588 (2001).
9. P. Yang, X. Tong, G. Wang, Z. Gao, X. Guo and Y. Qin, *ACS Appl. Mater. Interfaces*, **7**, 4772 (2015).
10. G. Wang, X. Peng, L. Yu, G. Wan, S. Lin and Y. Qin, *J. Mater. Chem. A*, **3**, 2734 (2015).
11. D. H. Kim, Y. J. Kim, Y. S. Song, B. T. Lee, J. H. Kim, S. Suh and R. Gordon, *J. Electrochem. Soc.*, **150**(10), C740 (2003).
12. T. S. Yang, W. Cho, M. Kim, K. S. An, T. M. Chung, C. G. Kim and Y. Kim, *J. Vac. Sci. Technol., A*, **23**(4), 1238 (2005).
13. E. Lindahl, M. Ottosson and J. O. Carlsson, *Chem. Vap. Deposition*, **15**, 186 (2009).
14. L. Yu, G. Wang, G. Wan, G. Wang, S. Lin, X. Li, K. Wang, Z. Bai and Y. Xiang, *Dalton Trans.*, **45**, 13779 (2016).
15. G. Wang, X. Peng, L. Yu, G. Wan, S. Lin and Y. Qin, *J. Mater. Chem. A*, **3**, 2734 (2015).
16. H. L. Lu, G. Scarel, C. Wiemer, M. Perego, S. Spiga, M. Fanciulli and G. Pavia, *J. Electrochem. Soc.*, **155**(10), H807 (2008).
17. H. L. Lu, G. Scarel, X. L. Li and M. Fanciulli, *J. Cryst. Growth*, **310**, 5464 (2008).
18. M. K. S. Barr, L. Assaud, Y. Wu, C. Laffon, P. Parent, J, Bachmann and L. Santinacci, *Electrochim. Acta*, **179**, 504 (2015).
19. P. Motamedi, K. Bosnick, K. Cui, K. Cadien and J. D. Hogan, *ACS Appl. Mater. Interfaces*, **9**, 24722 (2017).
20. Y. W. Kim and D. H. Kim, *Korean J. Chem. Eng.*, **29**(7), 969 (2012).
21. A. G. Hufnagel, A. K. Henß, R. Hoffmann, O. E. O. Zeman, S. Häringer, D. F. Rohlfing and T. Bein, *Adv. Mater. Interfaces*, **5**, 1701531 (2018).
22. D. Malwala and P. Gopinath, *Environ. Sci.: Nano*, **2**, 78 (2015).
23. R. K. Ramachandran, J. Dendooven and C. Detavernier, *J. Mater. Chem. A*, **2**, 10662 (2014).
24. J. H. Lee and J. H. Moon, *Korean J. Chem. Eng.*, **34**(12), 3195 (2017).
25. N. R. Chodankar, S. H. Ji and D. H. Kim, *J. Taiwan Inst. Chem. Eng.*, **80**, 503 (2017).
26. M. Zafar, J. Y. Yun and D. H. Kim, *Korean J. Chem. Eng.*, **35**(2), 567 (2018).
27. X. Chen, E. Pomerantseva, P. Banerjee, K. Gregorczyk, R. Ghodssi and G. Rubloff, *Chem. Mater.*, **24**, 1255 (2012).